Porous Silicon: Silicon Quantum Dots for Photonic Applications

L. Pavesi and R. Guardini
I.N.F.M. and Dipartimento di Fisica,
Università di Trento, via Sommarive 14, I-38050 Povo (Trento), Italy
email: pavesi@science.unitn.it - guardini@science.unitn.it

Received July 21, 1995

Porous silicon formation and structure characterization are briefly illustrated. Its luminescence properties are presented and interpreted on the basis of exciton recombination in quantum dot structures: the trap-controlled hopping mechanism is used to describe the recombination dynamics. Porous silicon application to photonic devices is considered: porous silicon multilayer structures in general, and microcavities in particular are described. The present situation in the realization of porous silicon LEDs is considered, and future developments in this field of research are suggested.

I. Introduction

With recent developments in communication systems and computer technology, the substitution of electrons with photons in data transmission and elaboration has become increasingly attractive. A great drawback is presented by the fact that silicon, the basic material for microelectronics, is an indirect-bandgap semiconductor which emits light in the infrared and at very low efficiencies (one photon emitted for every 10^7 photogenerated electron-hole pairs). One of the main directions of research in the field of photonic applications is to develop Si-based materials which emit light in the visible range efficiently and predictably: light emitting Si devices would in fact be cheaper than their counterparts made of compound semiconductors, and could also be integrated onto traditional circuits.

Among the many different Si-based materials studied for their luminescence properties, porous silicon (p-Si) has proved to be one of the most promising, as it emits light at room temperature in the visible range with quantum efficiencies approaching 10% (one photon emitted for every 10 photo-generated electron-hole pairs). p-Si was discovered by Uhlir in 1956[1], but its luminescence properties remained unnoticed until 1990, when they were reported by L.T. Canham[2]. Extensive research on luminescent p-Si has been promoted ever since.

The conclusions reached regarding its structure are generally accepted: the p-Si skeleton consists of interconnected Si nanocrystals of different sizes embedded in an amorphous matrix. Results of studies on the luminescence mechanism are not as clear, and divergent opinions exist on this issue. The debate is now focused upon three main models: the quantum recombination model, the surface state model and the molecular recombination model.

At the present stage, efficient photoluminescence (PL), and electroluminescence (EL) from p-Si with electrolytic contacts are commonplace phenomena, easily reproducible in the laboratory. On the other hand, strong EL from p-Si devices with solid-state contacts is still being sought after. p-Si Schottky diodes have been studied, yielding efficiencies of at most 10^{-4}%, and recently improvements on these values have been reported from p-Si p-n junctions[3].

Porous Si has been studied in Trento for the past four years: p-Si formation studies, characterization of its structure and luminescence investigation have all been conducted[4,5]. Recent work aims at the development of photonic applications. Multilayer p-Si structures have been created[6] and have been used to fabricate Bragg reflectors, Fabry-Perot filters and microcav-

ities. On the basis of past work on Schottky-type p-Si diodes[7], new structures are being investigated in order to achieve p-Si LEDs with improved performance.

This paper consists of three sections: the first section regards p-Si production and structure, mainly referring to the research work performed in Trento. In the second section the main luminescence properties of p-Si are outlined and interpreted in the light of the quantum confinement model. The trap-controlled hopping mechanism is presented to describe the recombination dynamics. The third section concerns photonic applications. A first part illustrates p-Si multilayer studies. A second is dedicated to p-Si LEDs: attempts to achieve a p-Si LED based on a Schottly diode are presented, together with the progress made with p-n junction devices. In conclusion, p-Si microcavity studies and their possible applications are illustrated.

II. Formation Mechanism

Porous silicon is made up of interconnected Si branches of nanometer size, which can be described in terms of quantum wires and dots. The quantum confinement effects which occur in these structures produce a widening of the band gap of p-Si with respect to crystalline Si (c-Si), in analogy to what happens in a simple particle-in-a-box example. A large amount of experimental evidence indicates that quantum confinement is responsible for p-Si's efficient luminescence over a wide band of the visible spectrum.

The creation of low-dimensionality systems usually involves sophisticated techniques[8,9]: p-Si fabrication, on the other hand, is a simple and cheap technique, based on the electrochemical attack of c-Si in a solution of hydrofluoric acid[10,11].

Current-voltage studies performed on Si-electrolyte junctions[12] show that the main requirements for p-Si formation are the following:

• the Si wafer must be anodically biased. This corresponds to forward biasing for p-type Si, reverse biasing for n-type Si.

• In the case of n-type and semi-insulating p-type Si, light must be supplied.

• Current densities below a critical value, j_{PS}, must be used.

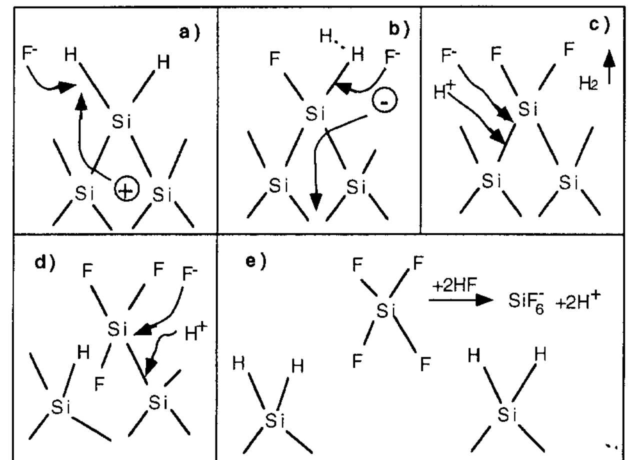

Figure 1: Diagram of the reaction mechanism for p-Si formation.

The first two conditions are due to the fact that holes are consumed during the dissolution (Fig. 1). When the third condition is violated, the reaction is limited by mass transfer to the solution: holes pile up at the Si-HF interface and electropolishing occurs.

All three requirements show that holes play an important role in the process: in fact, p-Si formation is a self-regulated mechanism, with hole depletion as the limiting agent. The dissolution reaction begins at defects of the Si wafer surface; pores are formed and their walls are eroded until they are emptied of holes. This passivates them from further attack, and the reaction proceeds at the pore tip (Fig. 2). The mechanisms which are thought to be responsible for hole depletion at the surface of the attacked wafer are two[12]. The first is a quantum confinement effect which occurs when feature size decreases below the dimensions of the Bohr radius of an exciton (∼5nm). The second is the formation of a depletion layer due to the Si electrolyte contact.

Together with the mechanisms of charge transfer across the Si-HF junction, hole depletion mechanisms determine feature size in the resulting p-Si layer. The quantum confinement effect yields *microporous* Si, with pore diameters below 2nm. When the depletion layer is thin, holes tunnel from Si to electrolyte; this leads to the formation of *mesopores*, whose diameter scales with depletion layer width and falls in the 2 to 50 nanometer range. With thicker depletion layers breakdown is responsible for charge transfer. Feature size goes from 50 nm to several μm and is independent of layer thickness.

These structures are termed *macropores.*

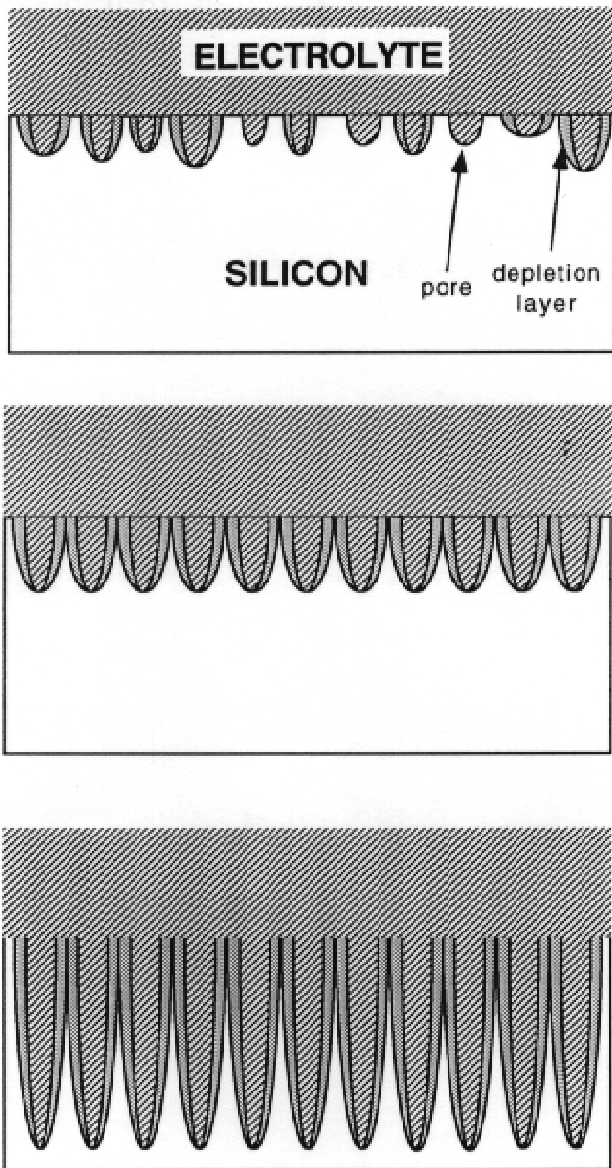

Figure 2: Steps in p-Si formation: a) pores are formed at the surface of the Si wafer. b) Their walls are thinned until they are depleted of holes. c) The reaction proceeds at the pore tips.

The type and concentration of dopants in the c-Si wafer employed in the attack determine the kind of p-Si which is formed. The first depletion mechanism is active in all types of Si. Under anodic bias, the depletion layer is nonexistent in low doped, p-type Si (p^- Si), is thin in highly doped Si both of p- and n-type (p^+ and n^+ Si respectively), and reaches thicknesses of a few μm in low doped n-type Si (n^- Si). Consequently p^- Si yields p-Si which consists entirely of micropores, which also coat the larger structures formed in the other types of Si. As light emission originates in microporous Si, samples made from p^- Si wafers have the best luminescent properties.

For a fixed wafer type, the thickness and porosity[1] of the resulting p-Si layer can be varied by modifying the values of the attack parameters employed for the electrochemical reaction. Porosity increases inversely with HF concentration, and directly with current density. Samples of porosity between 20% and 85% can be fabricated with ease. At higher porosities, the fragile Si skeleton is unable to withstand the large capillary forces which are present within the pores during drying, and samples craze and peel from the substrate. HF concentration determines j_{PS}, the upper limit to current density values. At a fixed, low HF concentration the range over which current density can be varied is short, and it becomes wider by increasing HF.

Layer thickness increases linearly with etch duration, if anodization time is not too long. Increasing HF concentration at fixed current density and etch time leads to thicker p-Si layers: this is due to the fact that the porosity decreases, while the amount of eroded material (proportional to the amount of charge exchanged) remains constant. For each porosity a limit thickness value exists, above which the p-Si layer detaches itself from the substrate. The structure of high porosity p-Si is fragile, so the limit thickness decreases with increasing porosity.

Experimental details for p-Si production: The setup used in Trento for p-Si formation is illustrated in Fig. 3. The electrochemical cell is made of Teflon and has a circular aperture on its bottom, under which the Si wafer is sealed. The working electrode (anode) of the reaction is the wafer itself, and the counter electrode (cathode) is made of platinum wire. A constant current is supplied to the system with a model 273 A EG&G PAR galvanostat. The electrolyte is formed by adding ethanol to a high purity aqueous solution of HF 40%. After the electrochemical attack, the samples are rinsed in methanol and blown dry with nitrogen. Wafers of p-type have been used, with the following dopant concentrations: 0.01 (p^+), 5, 10, 20 Ωcm (p^-). An Al film was deposited on the back of the p^- samples by sputtering and sintered at 400°C to ensure a good ohmic contact: the 20 Ωcm wafers had to be implanted with B atoms prior to Al deposition to improve the ohmic

[1] The porosity is defined as the ratio of dissolved material to attacked material, and gives an idea of structure size in the p-Si layer: samples of increasing porosity present thinner and more fragile Si skeletons, which contain smaller nanocrystals.

contact and avoid the formation of inhomogeneous p-Si layers.

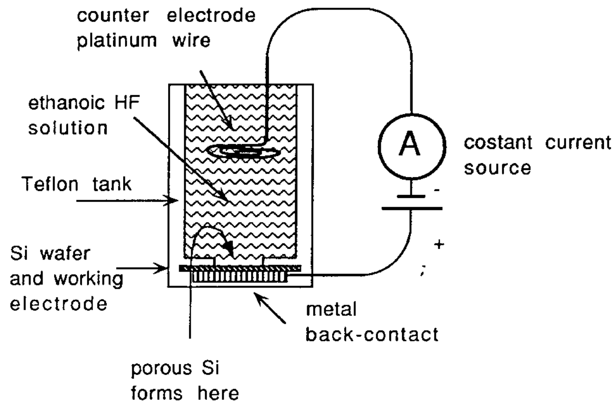

Figure 3: A typical set-up for p-Si formation.

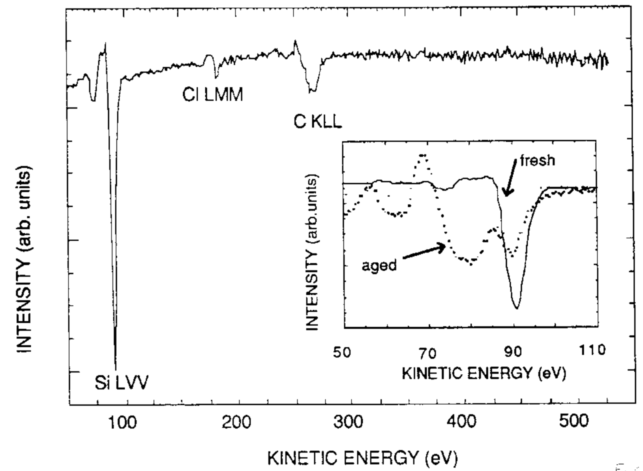

Figure 4: Auger survey acquired at the surface of a p-Si sample. The inset shows the Si Auger lineshape relative to freshly etched (continuous line) and aged (discs) p-Si. Reprinted from Ref [4].

III. Structure characterization

Within our research project, many different characterisation techniques have been used to gather information on p-Si structure. A combination of Auger, Raman, IR, EXAFS and Electron Paramagnetic Resonance (EPR) measurements have yielded the most important results, and are described in detail in previous work[5,13−16]: in this paper, the results are outlined briefly, to illustrate the model of p-Si structure.

The typical Auger spectrum of a freshly etched p-Si sample is shown in Fig. 4. Within the 50-530 eV energy range considered here, the Si LVV, CI LMM and C KLL transitions are observed. The lack of evidence for the O KLL peak, which should lie around 510 eV, is worth noticing. It proves that the thin native silicon oxide layer which is generally observed on Si surfaces is not present here. The Si LVV transition, shown on an expanded scale in the inset of Fig. 4, is the fingerprint of hydrogenated Si. These two facts prove that the Si dangling bonds at a freshly etched p-Si surface are passivated by H or, possibly, H and C containing radicals. The Auger spectrum of the same sample taken after ageing in atmosphere for a few weeks shows on the contrary the presence of the O KLL transition, together with the Si LVV lineshape characteristic of ionic bonded Si In a SiO_x complex[5]. The latter is also shown in the inset of Fig. 4.

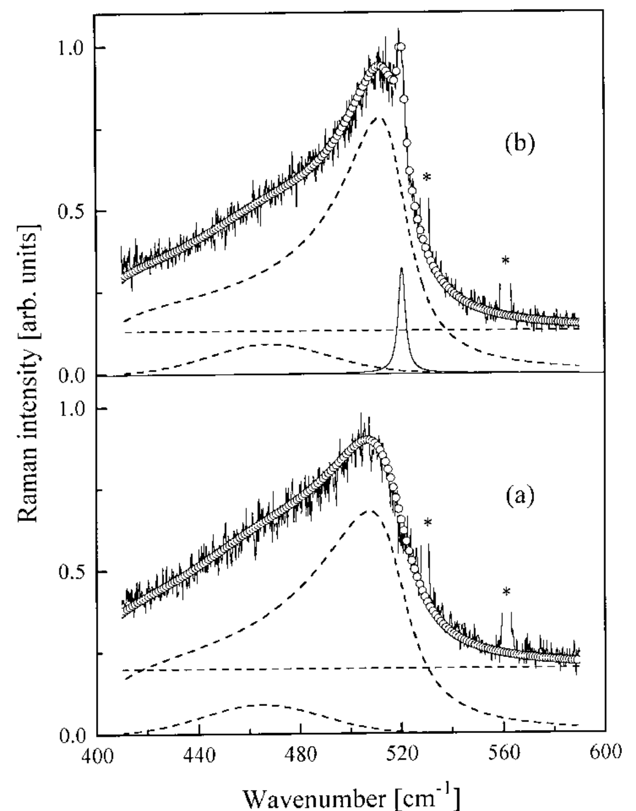

Figure 5: Room temperature Raman spectra excited at different depths within the cross section of a 15μm thick and 34% porosity p-Si sample. The stars label the position of two plasma lines used as energy standard. Spectrum (a) corresponds to a point near the interface air/porous layer while spectrum (b) to a point near the interface porous layer/bulk Si. The continuous lines refer to the experimental data and the open discs to a lineshape fit which considers the contributions of nanocrystalline Si, amorphous Si and of the underlying bulk Si. These three different contributions are shown as dotted lines. The figure is reprinted from Ref [13].

Room temperature micro-Raman spectra (Fig. 5) present a characteristic softening and broadening of the Si crystalline optical phonon mode, due to phonon confinement within the nanocrystals. A lineshape analysis has been conducted, assuming two main contributions to the spectrum: one due to an amorphous phase, with a Gaussian lineshape, and the other to nanocrystals, and fitted with the lineshape of Ref. [17]. This yields an asymmetric Lorentzian lineshape, whose peak position and linewidth are determined by nanocrystal size and shape[13].

EPR measurements were used to study the paramagnetic defects in p-Si. Dangling bond-type defects have been observed at the interface between the pore walls and an oxidised layer, and are thought to act as nonradiative recombination centres[16].

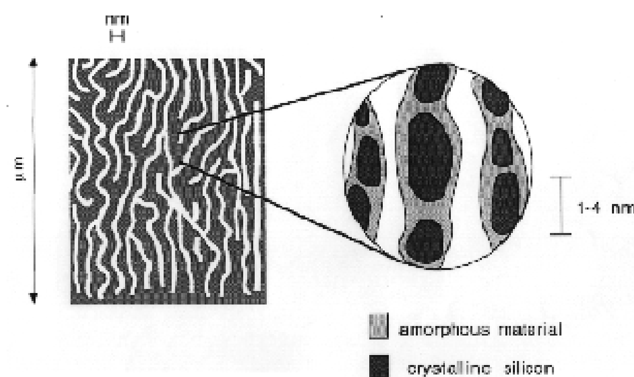

Figure 6: Model of p-Si structure: Si nanocrystals dispersed in an amorphous matrix.

The model of p-Si which emerges from these results is of a layer made up of voids and nanocrystals interconnected by an amorphous matrix (Fig. 6). Shortly after etching, this structure is passivated with hydrogen, which is replaced by oxygen as the sample ages in atmosphere. Strong evidence has been found of the presence of dangling bond defects at the surface of the nanocrystals. Short range crystallinity[15], passivation[14] and confinement[2] are all present in p-Si: both experimental and theoretical studies which have been conducted recently seem to indicate that these three factors combine to produce p-Si luminescence. The issue of light emission from p-Si is considered in the next section.

IV. Luminescence from p-Si

Porous silicon exhibits efficient room temperature luminescence in the visible range. Its spectrum is characterized by three main features: a blue band, the broad red-orange band which drew attention to p-Si in the first place, and an infrared band peaked at roughly 1 eV. The blue band can most likely be ascribed to emitting centres in the amorphous matrix[18]. Its intensity and peak position are sample dependent. EPR measurements and analogies with amorphous hydrogenated Si lead to think that the infrared band is due to the recombination of charge carriers trapped in the dangling bonds at the surface of the nanocrystals[19]. The mechanism responsible for p-Si's red- orange light emission is a matter of great controversy: the complexity in the structure of this material has led to the formulation of many different models to explain its luminescence. Basically they can be grouped into three categories:

1. quantum recombination model;
2. surface state model;
3. molecular recombination model.

The first two models agree on the fact that quantum confinement plays a fundamental role in p-Si luminescence, but they differ in their predictions about the origin of the luminescence. The former model ascribes it to the recombination of *excitons* within the nanocrystals, whereas in the latter *individual* (i.e., not coupled) charge carriers, which could be found either in a bulk nanocrystal state (extended state) or trapped in a surface nanocrystal state, recombine radiatively[20]. According to the third model, molecular species such as polysilane chains or siloxene rings are present in the amorphous phase of p-Si, and are responsible for the luminescence[21].

A large amount of experimental evidence has been gathered in favour of the first model[2,22]. X-ray studies have proved that the radiative recombination centres in p-Si are of crystalline origin[23,24]. The photoluminescence spectra reported in Fig. 7, which have been taken from samples of different porosities, show that the peak of the visible band shifts towards higher energies with increasing porosities. This is thought to be due to the fact that nanocrystals become smaller in samples of increasing porosity, and are thus characterised by wider band gaps. Another phenomenon in favour of the quantum confinement model is the blue shift of the PL peak which occurs when the sample ages in the atmosphere. With time the hydrogen which originally passivates the surface of the p-Si layer is replaced by oxygen, and the

amorphous layer surrounding the nanocrystals thickens at the expense of the inner crystalline part.

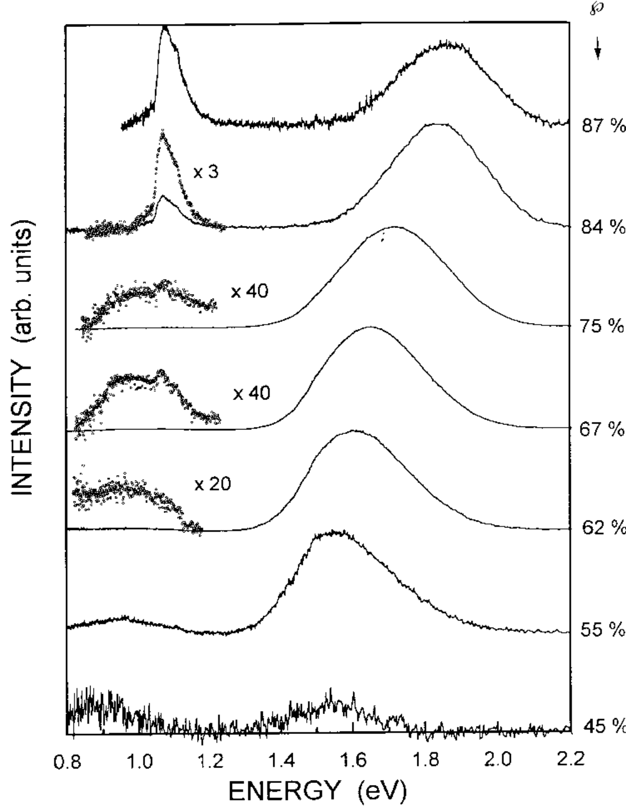

Figure 7: Room temperature photoluminescence spectra of a set of p-Si samples. The respective porosities are given on the right-hand side of the figure. On some spectra, the low energy part has been multiplied by the reported factors in order to evidence its contribution. The excitation energy and intensity were 2.54 eV and 1.6 Wcm^{-2}, respectively. The spectra are normalised to the maximum relative intensity and are not comparable with each other.

Further evidence was collected by our group during the course of an extensive experimental study on p-Si photoluminescence[5]. The results of this work, backed by Monte Carlo simulation studies, were used to formulate a model of the dynamics of exciton recombination in nanocrystals: the trap-controlled hopping mechanism. The model is described in detail, together with experimental and theoretical procedures, in Refs. [25, 26]: the main results and implications are illustrated in this paper.

P-Si luminescence is thought to originate from *exciton* recombination in *quantum dot* (QD) structures, *i.e.* in the nanocrystals. As a consequence of confinement, the exchange energy between triplet and singlet exciton states increases. In c-Si it is roughly 0.1 meV., whereas it becomes of the order of 10meV in p-Si. Recombination from the triplet state is a forbidden transition, with decay times of the order of milliseconds, while that from the singlet state is allowed, and has decay times in the microsecond range. When e-h pairs are formed in the nanocrystals, they relax to the QDs' fundamental energy levels on a fast time scale. At low temperature practically all excitons will find themselves in triplet states, while the occupation of singlet states will increase with increasing temperature. Consequently, the temperature dependence of the radiative lifetime ($\tau_{\rm rad}$) results from the thermal equilibrium between the exciton occupation of the triplet and singlet states:

$$\tau_{\rm rad}(E,T) = \tau_{\rm tripl}\left[\frac{1+\left(\frac{1}{3}\right)\exp\left(\frac{-\Delta E_x}{k_BT}\right)}{1+\left(\frac{\tau_{\rm tripl}}{\tau_{\rm sing}}\right)\left(\frac{1}{3}\right)\exp\left(-\frac{\Delta E_x}{k_BT}\right)}\right] \quad (1)$$

where $\tau_{\rm sing}$, $\tau_{\rm tripl}$ are the radiative lifetimes for the singlet and triplet states respectively, and ΔE_x the exchange energy. Temperature dependent lifetime measurements of the decay luminescence lineshape provide evidence for this interpretation, as will be illustrated later on in this section.

The decay lineshape of p-Si luminescence measured at a single observation energy is illustrated in Fig. 8. No single exponential will fit the experimental results well, whereas the data are in good agreement with a stretched exponential curve. The mathematical expression of the stretched exponential is:

$$I(t) = I(0)\cdot\exp[-(t/\tau)^{\beta}] \quad (2)$$

where $I(t)$ is the luminescence intensity at time t, τ is the decay lifetime and β is a dispersion exponent. This function represents the limiting sum over a distribution of exponential functions, each of which represents an elementary decay process: in p-Si, the distribution is thought to be due to the dispersive motion of excitons through the material.

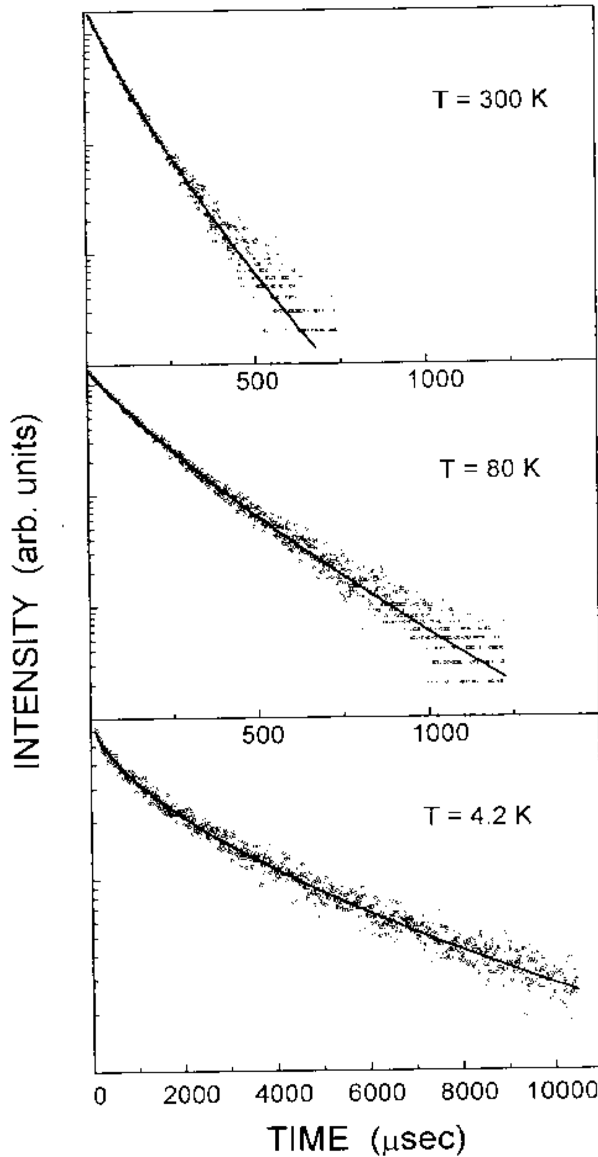

Figure 8: Time decay of the luminescence of a 60% porosity sample at three temperatures for E_{exc}=2.541 eV and E_{obs} =1.860 eV.

After excitation, the electron-hole pairs are involved in one of the following processes: (i) recombination in the quantum dot (QD) of origin through radiative channels; (ii) recombination through nonradiative channels; (iii) diffusion to neighbouring QDs. Disorder plays an important role both in the recombination and the diffusion processes. Nanocrystal size varies randomly within the p-Si skeleton; consequently QD recombination energies are distributed over a certain range. The random disposition of nanocrystals and the variations present in the composition of the amorphous matrix are reflected in variations of the inter-dot potentials and distances. This last factor gives rise to a random distribution of waiting times for diffusion due to hopping processes.

Measuring the decay lineshape at a specific observation energy corresponds to registering the luminescence of QDs of a certain size (target QDs). The disorder which characterizes the surroundings of the target QDs yields a distribution of the arrival times of excitons which were photocreated elsewhere and recombine here; The overall result is the stretched exponential lineshape which is observed experimentally.

Low energy QDs with high energy barriers and/or large separation distances from their nearest neighbours act as *temporary traps* for the excitons. They limit the diffusion, conferring it a dispersive character. Temperature has a strong effect on the dispersive diffusion. At low temperatures, the motion of excitons is dominated by temporary traps, while at high temperatures the traps are thermally emptied and the hopping mechanism prevails. In the latter situation the excitons thermalise among the QDs; their final distribution is determined solely by exciton energy and not by the environment around the QD which they occupy. When the temporary traps are activated, complete thermalisation does not occur. In this case the environment of each QD determines whether it is occupied or not, rather than its transition energy.

According to this model for exciton diffusion, β and τ can be interpreted as follows: the value of β indicates how far the system is from the isolated QD model and gives information on the mechanism which governs exciton motion among the QDs. τ can be roughly approximated by the expression:

$$\tau^{-1} \approx \tau_{\mathrm{rad}}^{-1} + \tau_{\mathrm{nr}}^{-1} + \tau_{\mathrm{hop}}^{-1} \qquad (3)$$

where τ_{rad}^{-1} is the radiative lifetime, τ_{nr}^{-1} the nonradiative lifetime and τ_{hop}^{-1} a characteristic hopping time: the role of diffusion is to reduce the time constant of the observed luminescence decay.

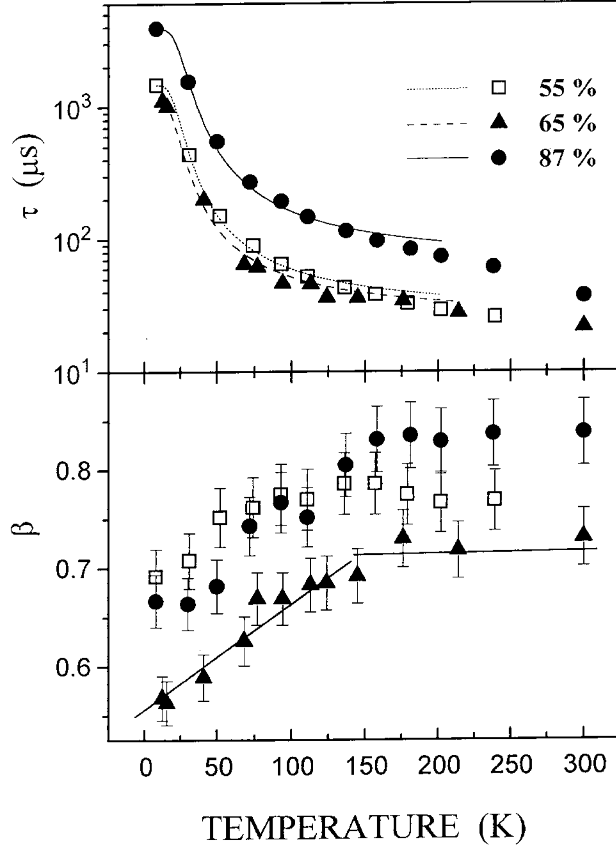

Figure 9: Temperature dependence of τ and β for three different samples, whose porosities reported on the right hand side. The lines through τ values are least square fits to Eq.1 with the following values: 87% sample, τ_{singl} = 17.8μs, τ_{tripl} = 3.90ms, ΔE_x=10.0meV; 65% porosity sample, τ_{singl} = 6.24μs, τ_{tripl}=5.89ms, ΔE_x=9.4meV, 55% sample, τ_{singl} = 5.89μs, τ_{tripl}=1.12ms, ΔE_x = 8.7meV. The lines through the β values are only guides for the eyes.

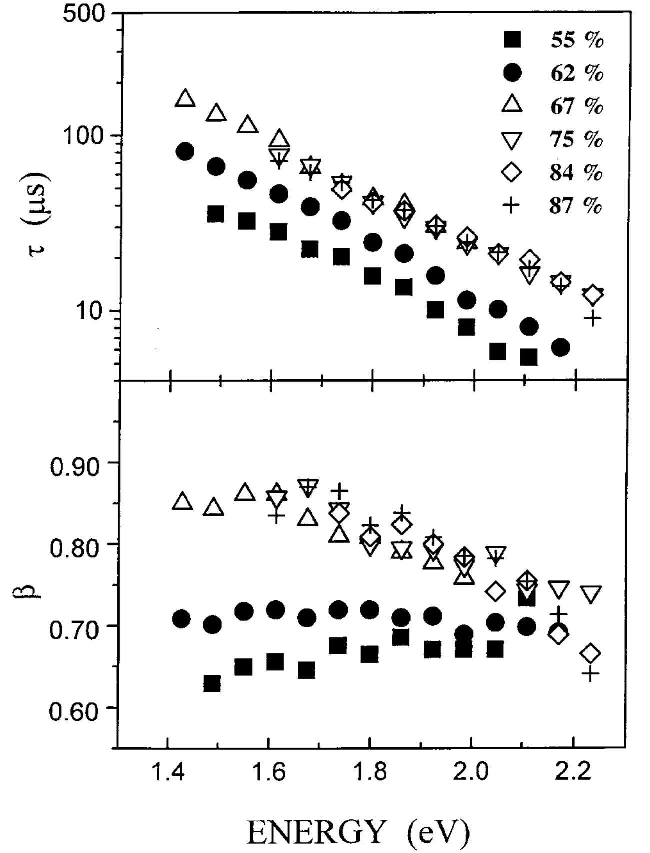

Figure 10: Observation energy dependence of τ and β for different samples whose porosities are reported on the right hand side.

The stretched exponential function has been used to fit experimental PL time-decay curves. Measured data are well described by the theoretical expressions, and reliable values of β and τ have been obtained. The influence on these two parameters of several factors has been studied experimentally and compared with theoretical predictions[26]. The temperature and porosity dependencies of β and τ are illustrated in Figs. 9 and 10, and can be interpreted as follows. *τ and β versus T:* Fig. 9 shows the temperature dependence of τ and β for three samples of different porosities. A trend common to all samples in both τ and β is observed: τ decreases strongly as T is increased, while β increases for $T < 150$K and is constant at higher temperatures.

At low and intermediate $T (T < 200\text{K})$ hopping is reduced and nonradiative transitions are not competitive. Consequently, T reflects the behaviour of the lifetime for the radiative recombination, τ_{rad}^{-1} which is given in Eq. 1. This confirms the assumption of excitonic recombination in the QDs. For higher temperatures ($T > 200$K), the observed decrease in τ is due to the competing role of non-radiative recombinations.

The temperature dependence of β gives information on the relative importance of the different models of transport among QDs. If β increases linearly with temperature, the multi-trapping mechanism applies for dispersive transport. On the contrary if β remains constant for T variations, the hopping mechanism dominates. The former regime is encountered below 150K, and indicates the T range in which temporary traps play an important role. The latter is entered for $T > 150$K; the temporary traps are thermally emptied here, and geometrical arrangement limits the diffusion. τ and β versus porosity: τ and β are plotted as a function of observation energy (E_{obs}) in Fig. 10

for samples of various porosities. In both plots, a low porosity and high porosity regime can be seen. Values of high porosity samples all lie on the same exponential curve, *i.e.* the measured lifetimes depend on $E_{\rm obs}$ only. This indicates that in these samples the QDs are almost isolated ($\tau_{\rm hop} \simeq \infty$) and τ depends mainly on the properties of the target QDs, and not on their surroundings. The lifetimes measured for low porosity values are smaller and sample dependent. This can be attributed to the presence of a network of interconnected QDs, among which excitons diffuse: the recombination is now influenced by the environment of the target QDs, and τ decreases due to the finite contribution of $\tau_{\rm hop}$. The reason for the different behaviour of excitons in low and high porosity samples can be found in the fact that high porosity samples have lower interconnections, and are more efficiently passivated with a thick amorphous surface layer which strongly reduces the hopping probability among different QDs. Further proof of this is given by the measured β values. As explained earlier, β indicates how far the system is from the isolated QD picture: the lower the β values, the better the interconnections among the neighbouring QDs.

In conclusion, many aspects of p-Si luminescence are well described in terms of exciton recombination in quantum dots. Disorder plays an important role in the process, and rules the motion of excitons between QDs as explained by the trap-controlled hopping mechanism. Monte Carlo calculations based on this model reproduce experimental results to a good extent[25]; it is worth mentioning that this is not the case for calculations based on the motion of uncoupled electrons and holes among the nanocrystals. This underlines the excitonic nature of the particles responsible for the luminescence.

V. p-Si applications to photonic devices

Multilayer structures: One of the main results of our recent work has been to fabricate and optically characterise dielectric p-Si multilayers[6]. These are complex p-Si structures formed by stacking layers of different porosities. In p-Si the refractive index, n, is related to porosity, so that in multilayers n varies periodically with depth. It is possible to create these structures thanks to the properties of the etch process: the dissolution reaction is *self-limited* so once a p-Si layer is formed, it is passivated from further attack, and thus other layers can be created beneath without damaging it. Si dissolution occurs *at the pore tips only*, and *abrupt porosity variations can be achieved* by modifying appropriately the attack parameters: this makes it possible to create planar layers with well-defined interfaces.

Multilayers can be used to create interferential filters and/or narrow band reflectors formed by dielectric films[27], with which it is possible to tune and narrow the p-Si emission band. In Trento high quality Bragg reflectors and Fabry-Perot filters have both been fabricated, and have proved to serve this purpose. Basing ourselves on the Fabry-Perot devices, we have succeeded in fabricating p-Si microcavities, which are made by sandwiching a p-Si layer of thickness λ, where λ is the wavelength of the Fabry-Perot high transmittance mode, between two distributed Bragg reflectors. Confinement of the emitted photons in the microcavity modifies the photon density of states[28], which leads to alterations in the spontaneous emission properties of the central p-Si layer. The consequences of the microcavity effect can be seen in Fig. 11. The reflectance and PL spectra of a p-Si microcavity are shown, and the PL data are compared with those of a reference sample. The most important features are a 16-fold increase in intensity and strong narrowing of the microcavity emission band. Further evidence of the microcavity effect is provided by angular resolved PL measurements, which show that the emission from the microcavity is strongly directional, and by time-resolved excitation spectroscopy, which shows a decrease in the luminescence decay time constant of a microcavity with respect to a p-Si monolayer, as predicted by theory.

Light emitting diodes: We have studied the electrical transport properties of p-Si by measuring the I- V characteristics of Schottky-type p-Si devices, fabricated by evaporating or sputtering a thin metal contact on top of a p-Si layer[7]. Initially, the experimental data (Fig. 12) were interpreted by considering the presence of a Schottky barrier between the p-Si and the metal contact. This yielded high series resistances and large ideality factors. Furthermore, the I-V characteristics proved to be independent of the type of metal used for the electrical contact. The measurements were better described in terms of the alternative description sug-

gested by M. Ben Chorin[29], in which the charge transport properties of p-Si dominate the I-V characteristics of the metal/p-Si diode. These can be tuned from poor rectifying behaviour for thin samples to nearly symmetric curves for thicker ones, which resemble very much a Poole-Frenkel type of transport. In this model, the device basically consists of a rectifying barrier located at the p-Si/c-Si hetero-interface, in series with a voltage dependent resistor, which is the porous layer. Charge transport within this layer is mainly due to hopping processes near the Fermi level, and is greatly influenced by the properties of the nanocrystallite surface and by the presence of deep trap states.

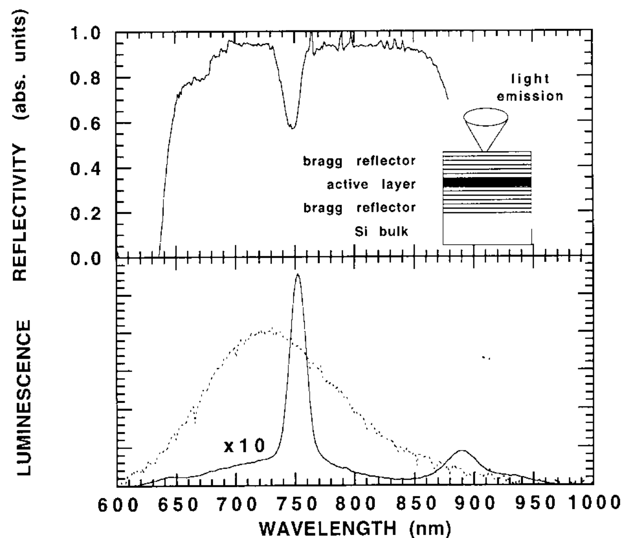

Figure 11: Microcavity reflectance and photoluminescence spectra (solid curve). The dotted line represents the photoluminescence spectrum of a reference sample.

Before p-Si can be employed in the production of photonic devices, efficient electroluminescence (EL) must be achieved. The external efficiency of the Schottky-type p-Si structures is orders of magnitude smaller than those of commercial LEDs. The main difficulties which have been encountered are the following: i) poor carrier injection; the intricate network of branches which make up p-Si is characterised by high resistance values. Furthermore, the evaporated metal layer on top of the p-Si is not uniform. Both these facts make it difficult to supply charge to the p-Si layer. ii) Fast time degradation of the EL: Light emission decreases with current flow over time intervals which range from a few minutes to several hours. Two factors are though to be responsible for this[3,5]: The first is the presence of islands in the metal layer, which act as point contacts. The heating effects caused by the high electric fields which build up here modify the structure of the p-Si. The second is a decay of the light emission itself. PL measurements performed on p-Si samples under the effect of electric fields show that current flow reduces the luminescence intensity. A likely explanation of this fact could be that the electric field promotes the creation of nonradiative recombination centres within the p-Si.

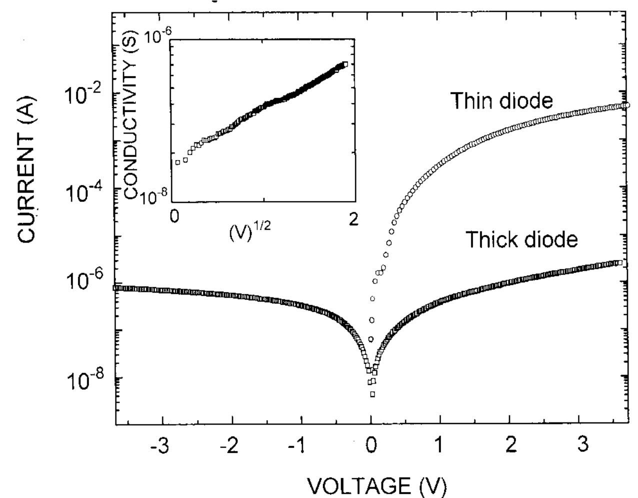

Figure 12: I-V characteristics of diodes with p-Si layers of different thicknesses. The discs refer to a $< 1\mu m$ thick diode, the squares to a $\approx 8\mu m$ thick diode. The metal contact was made of W. The characteristic of the thin diode is plotted only in forward bias for clearness. The inset shows the forward bias conductivity of the thick diode as a function of V^{12}.

Recently devices based on Si homojunctions have been created[3]; in these structures the electrons and holes are provided by the n- and p-t, type Si outside the porous region. This type of contact provides a more adequate carrier injection mechanism, and indeed these devices exhibit more efficient EL than metal Vp-Si structures, with slower degradation.

Further improvements could be achieved by incorporating a microcavity within the p-Si LED, which would benefit from the microcavity effects in the following ways: increase in light emission; narrowing of the spectral range; strong directionality of the emitted light.

A preliminary set of EL measurements (Fig. 13) performed in Trento showed an increase in EL intensity from a microcavity LED[30]. A second, unexpected result which was achieved was an increase in luminescence duration. This last effect could be due to the

fact that the emitting layer, i.e. the microcavity, is protected by the layers above. Further investigation in this phenomenon is needed to fully characterize these structures and optimize their fabrication.

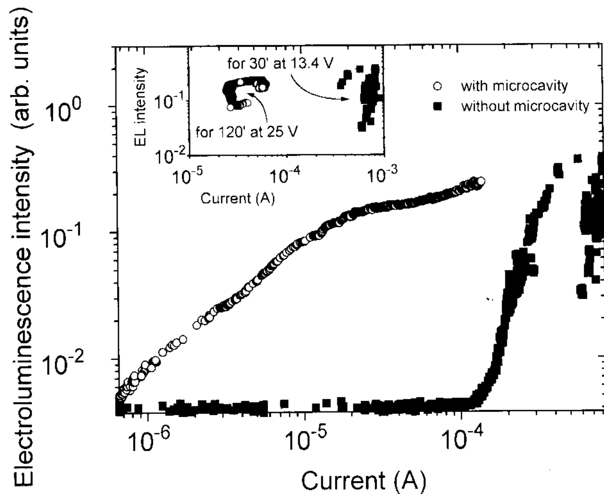

Figure 13: Electroluminescence intensity vs. current (EL-I) curves of a microcavity LED and of a standard metal/p-Si LED. Both curves are measured for increasing bias voltage. The inset shows the EL-I curves of the two devices measured at a fixed voltage bias. Note the greater stability of the microcavity LED. Furthermore, to achieve equal EL intensity from the two systems, the standard metal/p-Si LED must be supplied a current which is ten times greater than the one needed by the microcavity LED.

VI. Conclusion

The results presented in this paper illustrate the stage reached in p-Si research studies. The fabrication process has been mastered, and can be controlled with a precision which allows the formation of complex multilayer structures. P-Si structure and its photoluminescence properties have been studied in detail. It is generally acknowledged that p-Si is made of nanocrystals embedded in an amorphous matrix; the latter issue, on the other hand, is still under discussion. We have presented evidence which strongly supports the model of excitonic recombination quantum dots for the luminescence mechanism. Although the first p-Si based photonic applications are beginning to appear, a lot of work still has to be done in this field. Efficient EL production is one of the main aims: to achieve this, an efficient method to supply charge to the p-Si layer must be found; light emission must be maximized and stabilized. Homojunction devices are a possible solution to the first problem; microcavity incorporation in p-Si LEDs offers an attractive method to face the second.

Acknowledgements

It is a pleasure to acknowledge the fruitful and stimulating collaboration with O. Bisi and G. Mariotto, with whom many of the results presented here have been discussed and critically deepened. The hard work of the students M. Ceschini, G. Giebel, F. Ziglio and C. Mazzoleni is gratefully thanked. W. Theiss provided us with the refractive index and reflectance simulation program SCOUT. Other collaborators have been L. Calliari, F. Rocca, G. Dalba, A. Borghesi, A. Sassella, E.H. Roman, B. Pivac. The fine Si wafers used to produce p-Si were provided by dr. Rossetto of MEMC-Merano. This work is supported by the Italian National Council of Research (CNR) in the framework of the L.E. S. program.

References

1. A. Uhlir, Bell Syst. Tech. J. **35**, 333 (1956).
2. L. T. Canham, Appl. Phys. Lett. **57**, 1046 (1990).
3. P. Steiner, F. Kozlowski, W. Lang, Appl. Phys. Lett **62**, 2700 (1993).
4. L. Pavesi, G. Mariotto, O. Bisi, M. Anderle, L. Calliari, *Physical Concepts and Materials for Novel Optoelectronic Device Applications II*, Ed. F. Beltram and E. Gornik, SPIE vol.1985 (1993) pg.632.
5. L. Pavesi, M. Ceschini, G. Mariotto, E. Zanghellini, O. Bisi, M. Anderle, L. Calliari, M. Fedrizzi, L. Fedrizzi, J. Appl. Phys. **75**, 1118 (1994).
6. L. Pavesi, C. Mazzoleni, A. Tredicucci and V. Pellegrini, Appl. Phys Lett. **67**, 3280 (1995).
7. G. Giebel, L. Pavesi, Physica Status Solidi (a) **151**, 355 (1995).
8. O. Dag, A. Keperman, G. A. Ozin, Advanced Materials **7**, 72 (1995).
9. S. S. Iyer, Y-H.Xie, Science **260**, 40 (1993).
10. *Porous Silicon*, edited by Zhe Chuan Feng and Huan Tsu (World Scientific publishing Co., New York 1995).

11. Special issue of Journal of Luminescence vol. 57 (1993).
12. U. Gosele, V. Lehmann, in Ref [10], pag.17.
13. L. Pavesi, G. Giebel, F. Ziglio, G. Mariotto, F. Priolo, S. U. Campisano and C. Spinella, Appl. Phys. Lett. **65**, 2182 (1994), G. Mariotto, F. Ziglio, F. L. Freire Jr., J. Non-Cryst. Solidi, **192&193**, 253 (1995).
14. A. Borghesi, A. Sassella, B. Pivac, L. Pavesi, Solid St. Comm. **87**, 1 (1993), A. Borghesi, G. Guizzetti, A. Sassella, O. Bisi, L. Pavesi, Solid St. Comm. **89**, 615 (1994).
15. G. Dalba, P. Fornasini, M.Grazioli, R. Grisenti, Y. Soldo and F. Rocca, Physica B**208&209**, 559 (1995).
16. B. Pivac, B. Ravkin, L. Pavesi, Appl. Phys. Lett. **65**, 3260 (1994).
17. I. H. Campbell and P. M. Fauchet, Sol. St. CommurL, **58** (10), 739 (1986).
18. L. Tsybeskov, J.U.V. Vanydeshev and P.M. Fauchet, Phys. Rev. B **49**, 7821 (1994).
19. M. S. Brandt and M. Stutzmann, Appl. Phys. Lett. **63**, 2569 (1992).
20. F. Koch and V. Petrova-Koch, in Ref I10.], pag. 133, F. Koch, V. Petrova-Koch and T. Muschik, in Ref. [11], pag. 271.
21. M.S. Brandt and M.S. Stutmann, Solid St. Comm. **93**, 473 (1995).
22. P.D.J. Calcott, K.J. Nash, L.T. Canham, M.J. Kane and D. Brumhead, J. Phys: Condens. Matter **5**, L91 (1993); P.D.J. Calcott, K.J. Nash, L.T. Canham, M.J. Kane and D. Bmmhead in Ref [11], pag. 257.
23. S. Schupper et al., Phys. Rev. Lett. **72**, 2648 (1994).
24. T. K. Sham et al., Nature **363**, 331 (1993).
25. H.E. Roman and L. Pavesi, (to be published 1996).
26. L. Pavesi, J. Appl. Phys. (to be published 1996).
27. H. A. MacLeod, *Thin Film Optical Filters* (Adam Hilger Ltd., London 1969).
28. Y. Yamamoto, S. Machida, K. Igeta, G. Bjork, in *Coherence, Amplification and Quantum effects in Semiconductor lasers*, Ed. Y. Yammamoto (John Wiley & Sons, Inc., New York 1991) pag. 561
29. M. BenChorin, F. Moller and F. Koch, in Ref. [11], pag. 159; M. BenChorin, F. Moller and F. Koch, Phys. Rev. B**49**, 2981 (1994); M. BenChorin, F. Moller and F. Koch, J. Appl. Phys. **77**, 4482 (1995).
30. L. Pavesi, R. Guardini and C. Mazzoleni, Solid State Communications (1996).